S1. Supplementary Materials

S1.1. Equation of state

Our equation of state for the $MgSiO_3$ liquid follow the formulae previously derived (e.g., de Koker and Stixrude, 2009; Stixrude et al., 2009). The Helmholtz free energy is written as

$$F(V,T) = F_0 + F_{\rm cmp}(V,T_0) + F_{\rm th}(V,T), \tag{1}$$

where $F_0 = F(V_0,T_0)$ is the free energy at the reference volume, V_0, and temperature, T_0. $F_{\rm cmp}(V,T_0)$ and $F_{\rm th}(V,T)$ are the compressional and thermal contributions to the free energy, respectively. $F_{\rm cmp}$ is

$$F_{\rm cmp} = 9K_{T0}V_0\left(\frac{1}{2}f^2 + \frac{1}{6}a_3 f^3\right), \tag{2}$$

where

$$a_3 = 3(K'_{T0} - 4), \tag{3}$$

$$f = \frac{1}{2}\left[(V_0/V)^{2/3} - 1\right]. \tag{4}$$

K_{T0} is the isothermal bulk modulus (at $T = T_0$), and $K'_{\rm T0}$ is its pressure derivative at $p = 0$ and $T = T_0$. $F_{\rm th}$ is written as

$$F_{\rm th} = -\int_{T_0}^{T} S(V,T')dT'. \tag{5}$$

The entropy $S(V,T)$ is described as

$$S(V,T) = S_0 + \int_{V_0}^{V}\frac{C_V\gamma(V',T_0)}{V}dV' + \int_{T_0}^{T}\frac{C_V(V,T')}{T'}dT', \tag{6}$$

where $S_0 = S(V_0,T_0)$, and C_V is the specific heat that is assumed to be a constant. γ is the Grüneisen parameter, which is described as

$$\gamma = \gamma_0\left(\frac{V}{V_0}\right)^q, \tag{7}$$

where, γ_0 and q are constants.

The internal energy, E, and pressure, P, are described as

$$E(V,T) = E_0 + 9K_{T0}V_0\left(\frac{1}{2}f^2 + \frac{1}{6}a_3 f^3\right) + C_V(T-T_0) + C_V T_0 \int_{V_0}^{V} \frac{\gamma(V',T_0)}{V'}dV', \quad (8)$$

$$P(V,T) = 3K_{T0}(1+2f)^{5/2}(f + \frac{a_3}{2}f^2) + C_V(T-T_0)\frac{\gamma(V,T_0)}{V}. \quad (9)$$

Here, $E_0 = E(V_0, T_0)$. $\rho_0 = (1/V_0)$, T_0, K_{T0}, K'_{T0}, C_V, γ_0, q, E_0, and S_0 are listed in Table S1.

ρ_0(kg/m^3)	$T_0(K)$	K_{T0}(GPa)	K'_{T0}	C_V(J/K/kg)	γ_0	q	E_0(MJ/kg)	S_0(kJ/K/kg)
2650	2000	27.3	5.71	1480	0.6	-1.6	2.64	3.33

Table S1: Parameters for the $MgSiO_3$ liquid EOS.

S1.2. Mixing criterion

In a simple shear flow, the criterion for a Kelvin-Helmohltz instability (effectively the criterion for mixing) is $Ri \equiv N^2/(du/dz)^2 < 1/4$. Ri is the Richardson number of the system, N is the Brunt-Vaisala frequency, $N^2 \equiv -g(d\rho/dz)/\rho$, u is the velocity, z is the direction perpendicular to the flow, g is the gravity, and ρ is the density. Ri is related to the ratio of potential energy to kinetic energy (e.g., Taylor, 1931; Chandrasekhar, 1961) and is normally defined in terms of fluids with well defined constant density differences or a density gradient, but our system has variable values of all the input parameters. Therefore, we must necessarily restate the problem in terms of the energy budgets rather than explicitly in terms of velocity shear. The kinetic energy difference ΔKE per unit area for a layer of thickness L between the initial state (with shear) and the final state (with no shear but the same linear momentum) is

$$\frac{1}{2}\overline{\rho}\int_{-L/2}^{L/2}(u(z)^2 - (u_0/2)^2)dz = L\overline{\rho}u_0^2/24, \quad (10)$$

where u_0 is the initial velocity difference between the top and bottom and $\overline{\rho}$ is the mean density. The gravitational potential energy difference (ΔPE) between initial and final (fully mixed) states is

$$\int_{-L/2}^{L/2} (\overline{\rho} - \rho(z)) g z dz = \rho N^2 L^3 / 12, \tag{11}$$

where the density variation is assumed small. Therefore, the Richardson number criterion becomes ΔKE>2ΔPE and the physical interpretation is that one must provide not only the energy to overcome the potential energy difference but also the energy to mix (which shows up as heat from the dissipation of small scale turbulent motions). In the analysis provided by Chandrasekhar (1961) (p. 491), the ΔPE he defines is for complete overturn (that is, the new density profile is the exact opposite of the initial density profile), which is a different setting from ours. Therefore, his criterion differs from ours (mixed if $\Delta\text{KE} > \Delta\text{PE}$ in his anaysis).

S1.3. $MgSiO_3$ bridgmanite EOS

Figure S1 shows cross-sections of the mantles after the impact with the $MgSiO_3$ liquid and $MgSiO_3$ bridgmanite EOS. The thermodynamic parameters for the bridgmanite EOS is listed in Table S2. The entropy gains are slightly different, but the extent of shock-heating and the feature of $dS/dr > 0$ are similar among these cases. One might expect that a liquid mantle may gain higher entropy than a solid mantle based on the study done by Karato (2014). His work suggests that the surface of a molten mantle gains higher entropy by impact than a solid surface due to its smaller sound speed C_0 and negative q for the liquid (for the definition of C_0, see Section S1.5).

However, the difference in C_0 between the two EOS becomes smaller at a greater depth. This would diminish the difference between the entropy gained by the mantles with the two EOS. In addition, Karato (2014) use the Rankine-Hugoniot equations to describe the physics of the planetary surface, but we cannot use these equations to predict the entropy gain of the entire mantle as discussed in Section 4.1.

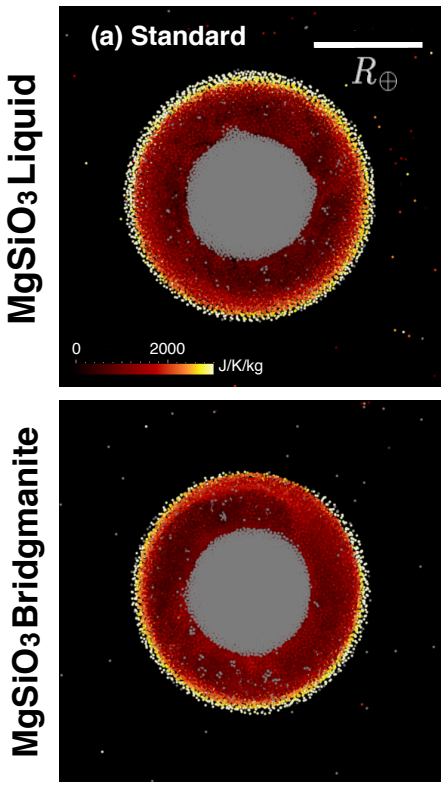

Figure S1: Entropy of the Earth's mantle after the impact. The top panel shows the case with the $MgSiO_3$ liquid EOS (this is the same as the top panel of Figure 2a) in the main text, and the bottom panel shows the case with the $MgSiO_3$ bridgmanite EOS.

ρ_0(kg/m^3)	$T_0(K)$	K_{T0}(GPa)	K'_{T0}	C_V(J/K/kg)	γ_0	q	E_0(MJ/kg)	S_0(kJ/K/kg)
3680	2000	200	4.14	1200	1.0	1.0	1.995	2.63

Table S2: Parameters for the equation of state of $MgSiO_3$ bridgmanite.

S1.4. Correction of the outer boundary

The density of the outer edge of the mantle is corrected because the simulation itself does not provide an accurate value. One of the reasons is that the standard SPH cannot describe a large density difference (e.g., CMB or planet-space boundary). The density of a particle at the outer boundary becomes too small because the particle does not have many nearby particles; thus, the smoothing length becomes large. This leads to a problem that dP/dr at the outermost part of the mantle becomes nearly 0 or it even becomes positive in (b) and (c) (Figure 3D). This state is not physically sensible because the hydrostatic equation is not correctly solved in the region.

To avoid this numerical problem, we define the minimum density $\rho_{\rm min} = \rho(r_{\rm max})$. Here, $r_{\rm max}$ is the maximum r whose region satisfies $dP/dr < 0$. If the density at $r > r_{\rm max}$ is lower, the r is recalculated by setting $\rho = \rho_{\rm min}$ and conserving the mass. Typically, $\rho_{\rm min} \sim 1500 - 1600$ kg/m^3 (Figure 3B). This is uncertain but may be reasonable because this is close to a rough estimate of the density at such a high temperature. The density at the outer edge can be approximated as $\rho \sim \rho_0(1 - \alpha T) \sim 1577$ kg/m^3 at $\alpha = 2.7 \times 10^{-5}$ (Fiquet et al., 2000), $\rho_0 = 2650$ kg/m^3, and $T = 1.5 \times 10^4$ K. After this procedure, ΔPE in the two EOS become similar. Thus, although this approximation is simple, it provides a reasonable answer.

S1.5. The Rankine-Hugoniot equations

Sugita et al. (2012) derive the following differential equations to describe after-shock temperature T and entropy S based on the Rankine-Hugoniot equations;

$$\frac{dT}{dU_p} = C_0\gamma_0 T\frac{(U_s - U_p)^{q-1}}{U_s^{q+1}} + \frac{sU_p^2}{C_V U_s}, \tag{12}$$

$$\frac{dS}{dU_p} = \frac{sU_p^2}{TU_s}. \tag{13}$$

Here, $p = p_i + \rho_i U_s U_p$ and $\rho = \rho_i U_s/(U_s - U_p)$, where p_i, ρ_i, U_s, and U_p are the pre-shock pressure, pre-shock density, shock velocity and particle

velocity. U_s and U_p has a relation $U_s = C_0 + sU_p$, where C_0 and s are the sound speed and constant. For our calculations, we choose $s = 1.56$ (for $MgSiO_3$ bridgmanite, Deng et al. 2008) and $T_i = 2000$ K (pre-shock temperature). At $p_i = 0$ GPa, $\rho_i = 4100$ kg/m^3, $C_0 = 6.47$ km/s and at $p_i = 50$ GPa, $\rho_i = 4500$ kg/m^3, $C_0 = 9.0$ km/s.

S1.6. Pressure vs. entropy increase

Figure S2 shows the relationship between the pressure (shown in grey) and entropy gain (shown in green). We choose a specific SPH particle from each simulation and track its properties. In (a), the primary impact, whose shock peak pressure is ~ 90 GPa, is the major source for the entropy increase. The entropy changes overtime, but the extent is limited. In (b), the SPH particle is heated by multiple shocks, including the primary impact-induced shock and shocks due to the planetary expansions and contractions (discussed in Section 4.1). After ~ 5 hrs, the entropy slowly increases due to continuous small-scale planetary deformation (the planet continues to wobble) until the system reaches its equilibrium state. In (c), the SPH particle experiences a number of shocks because the target and impact collide several times. The entropy gain is larger than the other two cases.

S1.7. Further discussions on the mixing analysis

We assume that the Earth's mantle was chemically heterogeneous before the impact, but here we further discuss its plausibility. Unlike (a) or (c), the model (b) requires that the Earth spins very quickly before the giant impact. This may indicate that the Earth experienced another (older) giant impact before the Moon-forming impact. This is because the angular momentum of a planet delivered by a number of small impacts from random directions tend to cancel out. This older giant impact could have been similar to the "sub-Earths" model, meaning that two similar mass objects collided, because this type of an impact is one of the easiest ways to deliver a large angular momentum to the planet (Canup, 2014). If this is the case, Earth's mantle could have been homogenized before the Moon-forming impact. If the heterogeneity formation predated this older impact, this could be a potential problem for (b). Alternatively, it is also possible that the heterogeneity formed between this older and the Moon-forming giant impacts, possibly in the form of a basal magma ocean by fractional melting and crystallization processes. The re-establishment of a compositionally distinct basal magma ocean could have been accomplished in less than 10^6 yr compared to the likely

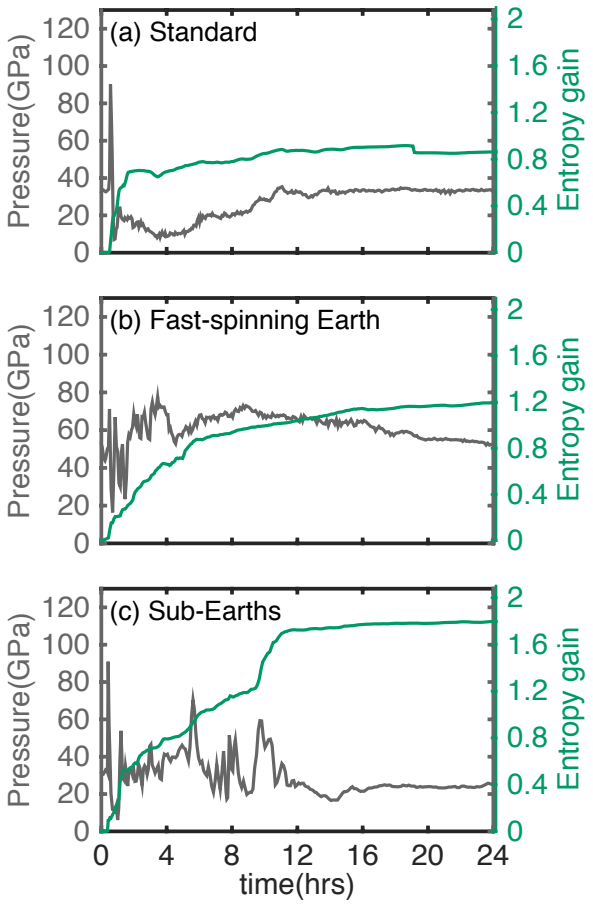

Figure S2: Time dependence of the pressure and entropy (in 10^3 J/K/kg) of an SPH particle in each model during the initial 24 hours.

time between giant impacts plausibly $\sim 10^7$ years (without an atmosphere, the majority of the mantle could have crystallized as short as 10^3 years, Solomatov 2000). It should be noted that there is no reason to suppose that this older impact was immediately prior, but the time interval might have been preferably short if the older impact formed a satellite. This is because the interaction between the Earth and satellite may have slowed the Earth's spin rate within $10^6 - 10^7$ years (Canup, 2014). This older satellite might have merged with a newer satellite formed by the last giant impact (Citron et al., 2014).

Another potential problem is that the critical value 0.5 has been derived to analyze the stability of horizontally stratified layers, but the value can differ for spherically stratified layers, as in our model. However, there is no literature concerning this geometry; thus, we simply apply the critical value for our analyses. The choice of the minimum density could also affect the estimate of ΔPE.

Furthermore, we only perform one simulation for each model and EOS. It is possible that ΔKE and ΔPE can change even for the same type of impact depending on the choice of the initial conditions (e.g., $v_{\rm imp}$ and b). To perform a simple and crude analysis, here we assume that the planetary kinetic energy is expressed as $\frac{1}{2}I\omega^2$, where I is the moment of inertia and ω is the angular velocity of the planet, and that I and ΔPE do not vary in the same model. We compute the ratio of ΔPE/ΔKE based on ω from published successful simulations (Ćuk and Stewart, 2012; Canup, 2012) and find that most of these simulations do not change the ratio large enough to cross the critical value 0.5, except Run 14 ($M_{\rm i}/M_{\rm T} = 0.45$, $b = 0.40$, and $v_{\rm imp}/v_{\rm esc} = 1.4$) in the sub-Earths model, depending on the EOS (0.52 for $MgSiO_3$ liquid and 0.38 for forsterite). Thus, our results likely provide the general trend, but some outlier may exist. Nevertheless, the choice of initial conditions is not likely to alter the signatures of $dS/dr > 0$ or the melting of the nearly entire mantle because these are states less sensitive to the conditions.

References

Canup, R. M., 2012. Forming a Moon with an Earth-like composition via a giant impact. Science 338, 1052–1055.

Canup, R. M., 2014. Lunar-forming impacts: processes and alternatives. Phil. Trans. R. Soc. A 372, 20130175.

Chandrasekhar, S., 1961. Hydrodynamic and hydromagnetic stability. Oxford Univ. Press, Oxford.

Citron, R. I., Aharonson, O., Perets, H., Genda, H., 2014. Moon formation from multiple large impacts. Lunar Planet. Sci. 45th, 2085.

Ćuk, M., Stewart, S. T., 2012. Making the Moon from a fast-spinning Earth: A giant impact followed by resonant despinning. Science 338, 1047–1052.

de Koker, N., Stixrude, L., 2009. Self-consistent thermodynamic description of silicate liquids, with application to shock melting of MgO periclase and MgSiO3 perovskite. Geophysical J. Int. 178, 162–179.

Deng, L., Gong, Z., Fei, Y., 2008. Direct shock wave loading of MgSiO3 perovskite to lower mantle conditions and its equation of state. Phys. Earth Planet. In. 170, 210–214.

Fiquet, G., Dewaele, A., Andrault, D., 2000. Thermoelastic properties and crystal structure of $MgSiO_3$ perovskite at lower mantle pressure and temperature conditions. Geophys. Res. Lett. 27, 21–24.

Karato, S., 2014. Asymmetric shock heating and the terrestrial magma ocean origin of the Moon. Proceedings of the Japan Academy, Series B 90, 97–103.

Solomatov, V. S., 2000. Fluid Dynamics of a Terrestrial Magma Ocean. Origin of the Earth and Moon. Univ.of Arizona Press, Tucson, pp. 323–338.

Stixrude, L., de Koker, N., Sun, N., Mookherjee, M., Karki, B., B., 2009. Thermodynamics of silicate liquids in the deep Earth. Earth Planet. Sci. Lett. 278, 226–232.

Sugita, S., Kurosawa, K., Kadono, T., Sano, T., 2012. An High-Precistion Semi-Analytical on-Hugoniot EOS for Geologic Materials. Lunar Planet. Sci. 43rd, 2053.

Taylor, G. I., 1931. Effect of Variation in Density on the Stability of Superposed Streams of Fluid. Proc. R. Soc. London A 132, 499–523.